R INRIA

INSTITUT NATIONAL DE RECHERCHE EN INFORMATIQUE ET EN AUTOMATIQUE

Coupled Geodesic Active Regions for Image Segmentation

Nikos PARAGIOS and Rachid DERICHE

N° 3783

Octobre 1999

THÈME 3

R apport de recherche

Coupled Geodesic Active Regions for Image Segmentation

Nikos PARAGIOS and Rachid DERICHE

Thème 3 — Interaction homme-machine,
images, données, connaissances
Projet Robotvis

Abstract: This paper presents a novel variational method for image segmentation which is obtained by unifying boundary and region-based information sources under the Geodesic Active Region framework. A statistical analysis over the observed density function (image histogram) using a mixture of Gaussian elements, indicates the number of the different regions and their intensity properties. Then, the boundary information is determined using a probabilistic edge detector, while the region information is given directly from the observed image using the conditional probability density functions of the mixture model. The defined objective function is minimized using a gradient-descent method where a level set approach is used to implement the resulting PDE system. According to the motion equations [PDE], the set of initial curves is propagated towards the segmentation result under the influence of boundary and region-based segmentation forces, and being constrained by a regularity force. The changes of topology are naturally handled thanks to the level set implementation, while a coupled multi-phase propagation is adopted that increases the robustness and the convergence rate by introducing a coupled system of equations for the different level set functions. Besides, to reduce the required computational cost and to decrease the risk of convergence to a local minimum, a multi-scale approach is also considered. The performance of our method is demonstrated on a variety of synthetic and real images.

Key-words: Image Segmentation, Maximum Likelihood, Geodesic Active Regions, Level Set Theory, Multi-phase Propagation, Multi-scale Segmentation.

e-mail: {nparagio,der}@sophia.inria.fr

http://www-sop.inria.fr/robotvis/personnel/{nparagio,der}/

Unité de recherche INRIA Sophia Antipolis
2004, route des Lucioles, B.P. 93, 06902 Sophia Antipolis Cedex (France)
Téléphone : 04 92 38 77 77 - International : +33 4 92 38 77 77 — Fax : 04 92 38 77 65 - International : +33 4 92 38 77 65

Couplage des Régions Actives Géodésiques pour la Segmentation d'Image

Résumé : Dans ce rapport, nous présentons une approche variationnelle pour traiter le problème de la segmentation d'image à l'aide du modèle de **Régions Actives Géodésiques** qui permet de prendre en compte de manière unifiée les informations liées aux régions et aux contours.

En premier, l'histogramme de l'image observée est approximé par une mixture de Gaussienne. Cette densité de probabilité est ensuite utilisée afin de déduire le nombre de régions et leurs propriétés statistiques. Les contours des régions sont ensuite caractérisés par une analyse statistique qui permet de définir une énergie qui inclut aussi bien un terme de région qu'un terme de contour. L'équation d'Euler-Lagrange associée à la minimisation de l'énergie est alors résolue à l'aide de la méthode des courbes de niveaux. Un ensemble de courbes initiales va ainsi se déplacer sous l'influence d'une contrainte de régularite et de forces associées aux contours et aux régions. Les changements de topologie sont naturellement traités grâce à la mise en oeuvre d'une approche à base de courbes de niveau. Afin d'augmenter la robustesse de l'approche et pouvoir par exemple segmenter aussi bien les éventuelles parties intérieures qu'extérieures des régions, nous proposons et développons une propagation multi-phase à base d'un système d'EDP couples. Afin de réduire le coût de calcul exigé, une approche multi-échelle est considérée. Plusieurs résultats expérimentaux, obtenues à partir de séquences d'images réelles, illustrent les diverses potentialités de cette approche.

Mots-clés : Segmentation d'image, régions actives géodésiques, théorie de courbes de niveau, propagation multi-phase, segmentation multi-échelle.

1   Introduction

The segmentation of a given image [15, 23, 27, 31], is one of the most important techniques for image analysis, understanding and interpretation. Besides, it is required as a low-level step to a large number of high level computer vision tasks.

Feature-based image segmentation is performed using two basic image processing techniques: the **boundary-based segmentation** (which is often referred as edge-based) relies on the generation of a strength image and the extraction of prominent edges, while the **region-based segmentation** relies on the homogeneity of spatially localized features and properties.

- Early approaches for **boundary-based** image segmentation have used local filtering techniques such as edge detection operators [6, 16]. These approaches are a compromise between simplicity, with accompanying light computational cost and stability under noise, but have difficulty in establishing the connectivity of edge segments. This problem has been confronted by employing Snake/Balloons models [14, 26] which can provide a closed curve as a compromise between regularity of the curve and high gradient values among the curve points. This type of approaches have been extensively used to deal with the image segmentation problem [21, 25]. Their main handicap is that they require a good initialization step. Recently, the geodesic active contour model has been introduced [7, 28] which combined with the level set theory [33] deals with the above limitation resulting in a very elegant and powerful segmentation tool.

  Although for many real cases the use of boundary-based segmentation methods are inappropriate, they provide some important advantages. Shape variations are naturally handled and they are not sensitive to global illumination changes due to the fact that they rely on relative illumination changes, rather than the absolute illumination intensities. Additionally, these methods require low computational cost and localize better the region/object boundaries.

- The **region-based** methods are more suitable approaches for image segmentation and can be roughly classified into two categories: The region-growing techniques [2, 4, 29, 43] and the Markov Random Fields based approaches [5, 17, 19]. The region growing methods are based on split-and-merge procedures using statistical homogeneity tests, where the statistics are generated and updated dynamically, while the manner with which initial regions are formed and the criteria for splitting and merging them are set *a priory*. The resulting segmentation will inevitably depend on the choice of initial regions, while irregularities on the boundaries will appear since the region shapes depend on the particular growing algorithm. Another powerful region-based tool, which has been widely investigated for image segmentation, is the Markov Random Fields (MRF) [20]. In that case the segmentation problem is viewed as a statistical estimation problem where each pixel is statistically dependent only on its neighbors so that the complexity of the model is restricted. The segmentation is obtained by finding the maximum *a posteriori* map given the observed data. The main advantage

of this type of approaches is that they are less affected from the presence of noise, and provide a global segmentation criterion. The optimization problem turns to be equivalent with the minimization of a global objective function and is usually performed using stochastic (Mean-field, Simulated Annealing) or deterministic relaxation algorithms (Iterated Conditional Modes [3], Highest Confidence First [12]). Although the MRF-based objective function is a very powerful model, usually it is time consuming (especially when the solution space is large), which might be perceived as a handicap.

- Finally, there is a significant effort **to integrate boundary-based with region-based segmentation approaches** [9, 13, 22, 36, 37, 39, 42, 43]. The difficulty lies on the fact that even though the two modules yield complementary information, they involve conflicting and incommensurate objectives. The region-based methods attempt to capitalize on homogeneity properties, whereas boundary-based ones use the non-homogeneity of the same data as a guide.

In order to better introduce the proposed approach and to demonstrate the new key issues with respect to the existing ones, some of the most representative as well as most closely related segmentation approaches with the one proposed in this section, are following.

Kass, Witkin and Terzopoulos in [26] have proposed the snake model for image segmentation, that aims at minimizing a curve-based objective function towards a regular curve that is attracted by pixels with important gradient values. *Cohen* in [14] has proposed a modification of the snake model by adding a pressure force that helps it to avoid local minima. Finally, *Caselles, Kimmel and Sapiro* in [8] and *Kichenassamy et al* in [28] have proposed the geodesic active contour model, which combined with the level set theory overcomes a large number of limitations imposed by the classical snake model and provides a powerful tool for image segmentation. A similar model (implemented within the level set framework) that is based on a geometric-based minimization approach was proposed by *Malladi, Sethian and Vemuri* in [30].

Beveridge et al in [4] have proposed a region growing segmentation algorithm that makes use of local histogram picks to determine the number and the form of the initial regions. Then, this number is decreased by performing a region growing phase. This method has been successfully exploited to deal with multi-modal/multi-feature data.

Adams and Bischof in [2] have proposed a seeded region-growing algorithm for image segmentation. Their approach is based on region growing but is also very close to the watershed mechanism. The region growing is controlled using a small number of pixels that refer to the seeds, and can provided very satisfactory results without involving many parameters.

Leonardis, Gupta and Bajcsy in [29] have proposed a method for segmenting range images into planar and second order surfaces. This approach consists of two steps; the model-selection and the model-recovery, that are solved sequentially within an iterative procedure where partially recovery of the models is followed by model selection (optimization procedure) that rejects the "weak" models. This interactive sequentially procedure is performed until convergence.

Derin et al in [17], have proposed a recursive MRF-based segmentation algorithm. This algorithm makes use of a Bayes smoothing operation that yields to the *a posteriori* distribution of the real scenes (segmentation) values given the noisy image. However, the assumption that the given image is corrupted by white noise constrains the model applicability.

Geiger and Yuille in [19], have proposed a Bayesian framework that unifies several approaches of image segmentation. This approach is implemented in the context of Markov Random Fields, where a very flexible objective function is defined that can be transformed to several well known image segmentation techniques by modifying its parameters. This method is quite general and seems to have an impressive performance.

Haddon and Boyce in [22] have proposed a two-stage segmentation method. An initial pixel classification is obtained by analyzing the distributions of the co-occurrence matrices. The local consistency of pixel classification is then implemented and updated by maximizing the entropy of local information, where region information is expressed via conditional probabilities, which are estimated from the co-occurrence matrixes. Additionally, the boundary information is expressed via conditional probabilities, which are determined *a priori*.

Pavlidis and Liow in [36] have proposed a method that combines region growing and edge detection for image segmentation. The first stage of this approach relies on a split-and-merge algorithm that aims at providing an over-segmented result. Then, the output of the split-and-merge procedure is combined with boundary criteria and measurements resulting on the final segmentation map (during this step, the initial region boundaries are either modified, or totally eliminated).

Pentland in [37] has proposed a specific application that performs segmentation and modeling. This approach is divided into two stages. During the first stage the input image is segmented into convex components. The second stage relies on fitting parametric 3D deformable models to the segmented image. However, this approach has limited applicability set.

Bouman and Shapiro in [5], have proposed a multi-scale Bayesian formulation for image segmentation that minimizes the size misclassified regions and decreases drastically the required computational cost. Furthermore, the authors have proposed a method to determine optimally the model parameters.

Mumford and Shah in [32] have proposed a variational framework for segmenting an image into homogeneous regions. Their method combines three different aspects: the length of the hypothetical boundary, the gradient values among the boundary pixels and the difference between the given image and a smooth version of it. Additionally, a regularity constraint is imposed for the boundary.

Chakraborty et al in [9], have proposed a technique that integrates gradient and region information within a deformable boundary finding framework. *Zhu and Yuille* in [43] have proposed a statistical variational approach which combines the geometrical features of a snake/balloon model and the statistical techniques of region growing. This approach has been recently implemented with the level set framework in [40].

Samson et al in [38] have proposed a supervised classification model that aims at finding a partition composed of homogeneous regions. They assume that the number of classes
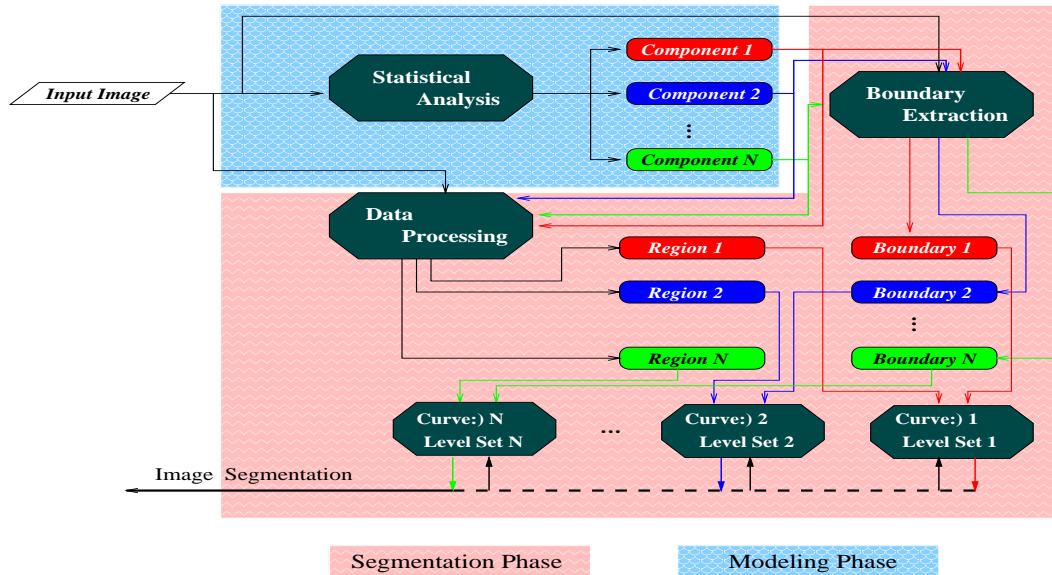
Figure 1: Multi-phase Coupled Geodesic Active Regions for Image Segmentation: **the flow chart**.

as well as their intensity properties are known, and formulate the classification problem using a variational framework, that aims at propagating mutually exclusive regular curves towards the different classes. The curve propagation is implemented using the level set theory. However, this model assume important prior knowledge, is very sensitive to the initial conditions and does not make use of any "edge"-based information.

A similar framework is proposed by *Chan and Vese* in [10]. This model follows the same principle with the one in [38] but is constrained by a bi-modal assumption, where the input image is assumed to be a synthesis of two classes. However, this model deals with the un-supervised image segmentation case, where there is no need of *a priori* knowledge. Similarly with the approach in [38], the curve propagation is implemented using the level set theory. This model is sensitive to the initial curve conditions and does not make use of any "edge"-based information.

Here, we will present a unified approach for image segmentation that incorporates boundary and region information sources under a curve-based minimization framework. This framework is exploited directly from the **Geodesic Active Region** [34, 35] model and presents some very nice properties. This approach is depicted in [**fig.** (1)].

The first stage refers to a modeling phase where the observed histogram is approximated using a mixture of Gaussian components. This analysis denotes the regions number as well as their statistics, since a Gaussian component is attached to each region. Then, the

segmentation is performed by employing the Geodesic Active Region model. The different region boundaries are determined using a probabilistic module by seeking for local discontinuities on the statistical space that is associated with the image features. This information is combined with the region one, which is expressed directly from conditional probabilities, resulting in a geodesic active region based segmentation framework. The defined objective function is minimized with respect to the different region boundaries (multiple curves) using a gradient descent method, where the obtained equations are implemented using the level set theory. Moreover, the set level set equations are coupled by demanding a non-overlapping set of curves since each pixel of the image cannot belong to more than one region. The resulting model deals automatically with the changes of topology thereby allowing either several sub-regions with the same intensity properties to be the output of a single initial curve, or a single curve to be the output of multiple initial curves. Finally, the objective function is used within the context of a coarse to fine multi-scale approach that increases the convergence rate and decreases the risk of converging to a local minimum.

The reminder of this paper is organized as follows. In section 2 the problem of determining the number of regions and their intensity properties is considered, while in section 3 a Geodesic Active Region-based approach for image segmentation is proposed. The implementation issues of this approach are examined in section 4, while the coupling between the different level set functions is introduced in section 5. Section 6 contains the final form of the proposed segmentation paradigm that is considered in a multi-scale approach presented in section 7. Finally, conclusions and discussion appear in section 8.

2   Regions and their Statistics

In order to simplify the notation and to better and easier introduce the proposed model, let us make some definitions:

- Let I the input image, and let $H(I)$ be the observed density function (histogram) of this image,

- Let $\mathcal{P}(\mathcal{R}) = \{\mathcal{R}_i : i \in [1, N]\}$ be a partition of the image into N non-overlapping regions, and let $\partial\mathcal{P}(\mathcal{R}) = \{\partial\mathcal{R}_i : i \in [1, N]\}$ be the region boundaries,

- And, let h_i be the segmentation hypothesis that is associated with the region $\mathcal{R}_i$.

The key hypothesis that is made to perform segmentation relies on the fact that the image is composed of homogeneous regions. This can be easily projected to the probability density space that is associated with the image features (histogram) by assuming that each region is represented to the observed density function with a Gaussian element.

Let $p()$ be the probability density function with respect to the intensity space of the image I (determined directly from the histogram $H(I)$). If we assume that this probability density function is homogeneous, then an intensity value x is derived by selecting a component k

with *a priori* probability P_k and then selecting this value according to the distribution of this element $p_k()$. This hypothesis leads to a mixture model of Gaussian elements

$$
\begin{cases}
p(x) = \sum_{k=1}^{N} P_k \ p_k(x) \\[2mm]
p_k(x) = \dfrac{1}{\sqrt{2\pi}\sigma_k} e^{-\frac{(x-\mu_k)^2}{2\sigma_k^2}}
\end{cases}
\tag{1}
$$

where

- N is the number of mixture components (regions number),

- P_k is the *a priori* probability of the component k,

- And $p_k()$ is the intensity probability density function that is followed by the component k.

This mixture model consists of a vector Θ with $3N+1$ unknown parameters $\Theta = \{(P_k, \mu_k, \sigma_k) : k \in [1, ..., N]\}$:

- The number of components $[N]$,

- The *a priori* probability of each component $[P_k]$,

- And, the mean $[\mu_k]$ and the standard deviation $[\sigma_k]$ of each component.

Hence, there are two key problems to be dealt with: the determination of the components number, and the estimation of the unknown parameters Θ of these components. The component number is derived automatically from the observed density function by looking for local maxima that initially correspond to the mean intensity values within the different regions.

Thus, the observed probability density function (discrete image histogram) is sorted according to the probability values and is processed hierarchically as follows:

> **i.** The most probable un-processed intensity value is considered,
>
> **ii.** **if** this value corresponds to a local maximum (histogram peak),
>
> > **then** it is considered as an eligible mean value.
> >
> > > **if** it presents a certain distance from the already selected mean values,
> > >
> > > > **then** the component number is increased by one and the candidate value is added to the initial set of components.
> > >
> > > **else** go to step i.
> >
> > **else** go to step i.
>
> **iii.** **if** there are still un-selected values, then go to step i.

To depict the above flow-chart, an intensity value is selected as a candidate component mean value if it refers to a local maximum and satisfies a distance constraint with respect to the already selected ones [1].

Then, given the component number and an initial estimation of the unknown parameters [2], the final estimation is obtained using an iterative scheme that is derived from the Maximum Likelihood Principle [18] where the parameter vector $(\hat{P}, \hat{\Theta})$ is the value of $(\hat{P}, \hat{\Theta})$ that maximizes the joint density.

Moreover, a correction step is performed to the *a posteriori* estimates that eliminates the components with insignificant probability. Then, same principle is applied to re-estimate the parameter vector of the mixture model (the component number is decreased). The efficiency of the method is demonstrated in [**fig.** (2,6)].

3 Geodesic Active Regions for Image Segmentation

Given the region number as well their expected intensity properties, we can proceed to the segmentation phase of the proposed approach within the Geodesic Active Region model.

3.1 Setting the Boundary Information

The first demand of this model relies on extracting some information regarding the real boundaries of each region. This can be done by employing an edge detector, thus by seeking for high gradient values on the input image. Given the hypothesis that this image is

---

[1]An alternative choice is the selection of the components number manually, by the user. This can be done by employing a small distance constraint that gives a large number of initial components. Then, the requested number is reached by eliminating successively the component with the smallest *a priori* probability.

[2]The standard deviation values are estimated using the first and the second order density moments, while the assumption that all components are equally probable is used to determine the *a priori* probabilities.

(a)   (b)   (c)
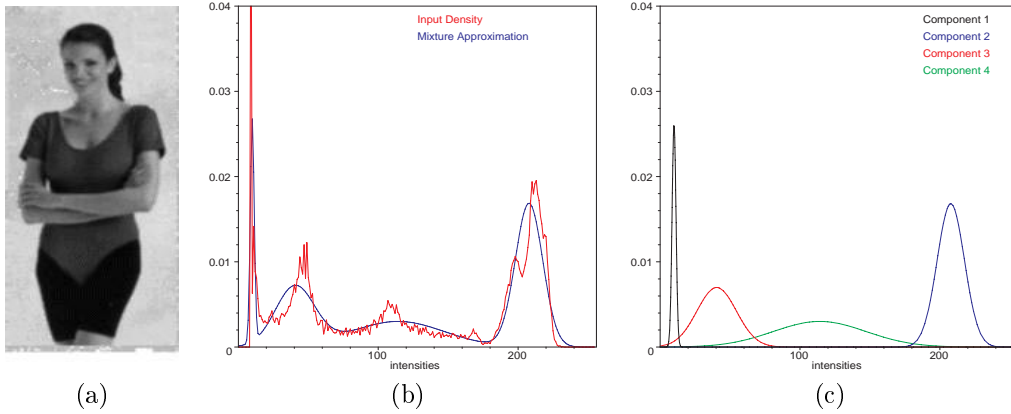
Figure 2: (a) Input Image, (b) Image Histogram and its approximation: *Components Number: 4, Mean Approximation Error: 1.04641e-05, Iterations Number: 117*, (c) Region Intensity Properties [*Component 1:* black pants, *Component 2:* background, *Component 3:* (hair, t-shirt), *Component 4:* skin].

composed of homogeneous regions, this method will provide reliable global boundary information. However, this information is blind, since its nature cannot be determined. In other words, a pixel with important gradient value (boundary pixel) cannot be attributed to the boundaries of a specific region $[\partial\mathcal{R}_i]$.

Here, an alternative method is proposed to determine the boundary-based information. Let s be a pixel of the image, $N(s)$ a partition of its neighborhood, and the $N_R(s)$ and $N_L(s)$ be the regions associated with this local partition. Moreover, let $p(B_k|I(N(s)))$ **be the boundary probability density function with respect to the k hypothesis**. This function measures the probability of a given pixel s with observed intensity values $I(N(s))$ in its neighborhood of being at the boundaries of the k region. Then, this probability is given by the Bayes rule as follows

$$p(B_k|I(N(s))) = \frac{p(I(N(s))|B_k)}{p(I(N(s)))}p(B_k) = \frac{p(I(N(s))|B_k)}{p(I(N(s))|[B_k]\cup[\bar{B}_k])}p(B) \qquad (2)$$

where

- $p(I(N(s))|B_k)$ is the **conditional boundary probability with respect to the k hypothesis** (s belongs to the k boundaries),

- $p(I(N(s))|\bar{B}_k)$ is the **conditional non-boundary probability with respect to the k hypothesis** (s does not belong to the k boundaries),
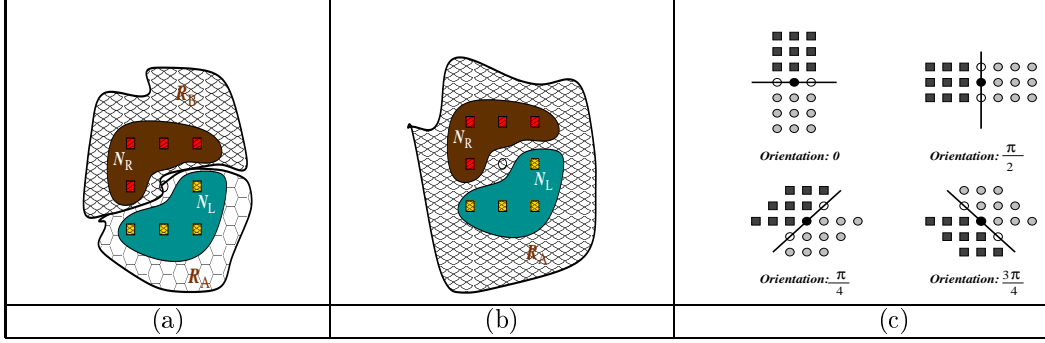
Figure 3: (a) Neighborhood partition that indicates a **boundary** point, (b) Neighborhood partition that indicates a **non-boundary** point, (c) Neighborhood partitions that are considered.

- $p(I(N(s)))$ is the probability of observing the neighborhood values $I(N(s))$ globally in the image. This probability can be determined by assuming that this neighborhood values either refer to a k boundary point s $[p(I(N(s))|B_k)]$, or to a non-k boundary point $[p(I(N(s))|\bar{B}_k)]$.

- Finally, $p(B)$ is the *a priori* boundary probability.

Due to the fact that the *a priori* boundary probability is a constant scale factor, it can be ignored. Moreover, the conditional boundary $[p(I(N(s))|B_k)]$ as well as non-boundary probability density function $[p(I(N(s))|\bar{B}_k)]$ can be estimated directly from known quantities. Thus, if s is a boundary pixel of the k hypothesis, then

k Boundary Condition [**fig.** (3.a)]:

i. Either there is a partition $[N_L(s), N_R(s)]$ where the most probable assignment for $N_L(s)$ is k and for $N_R(s)$ is $j, [j \neq k]$:

$$[N_L(s) \in \mathcal{R}_k \cap N_R(s) \in \mathcal{R}_j],$$

ii. Or, there exist a partition $[N_L(s), N_R(s)]$ where the most probable assignment for $N_L(s)$ is $j, [j \neq k]$ and for $N_R(s)$ is k:

$$[N_L(s) \in \mathcal{R}_j \cap N_R(s) \in \mathcal{R}_k].$$

Thus, the k conditional boundary probability can be estimated directly from known quantities as follows,

$$p(I(N(s))|B_k) = p\left([N_L(s) \in \mathcal{R}_k \cap N_R(s) \in \mathcal{R}_j] \cup [N_L(s) \in \mathcal{R}_j \cap N_R(s) \in \mathcal{R}_k]\,|I(N(s))\right)$$

$$= \underbrace{p_k(I(N_R(s)))\ p_j(I(N_L(s)))}_{N_R(s) \in \mathcal{R}_k \cap N_L(s) \in \mathcal{R}_j}\ +\ \underbrace{p_j(I(N_R(s)))\ p_k(I(N_L(s)))}_{N_R(s) \in \mathcal{R}_j \cap N_L(s) \in \mathcal{R}_k} \tag{3}$$

where

- $p_k(I(N_R(s)))$ is the probability of "right" local region $[N_R(s)]$ being at the k region, given the observed intensity values within this region $[I(N_R(s))]$,

- $p_j(I(N_L(s)))$ is the probability of "left" local region $[N_L(s)]$ being at the j region, given the observed intensity values within this region $[I(N_L(s))]$.

Moreover, if s is not a k boundary pixel [**fig. (3.b)**], then **for every possible neighborhood partition the most probable assignment for $N_L(s)$ as well as for $N_R(s)$ is either the k, or i and j where $\{i,j\} \neq k$.** As a consequence, the conditional k non-boundary probability is given by,

$$p(I(N(s))|\bar{B}_k) = p\left([N_L(s) \in \mathcal{R}_k \cap N_R(s) \in \mathcal{R}_k] \cup [N_L(s) \in \mathcal{R}_i \cap N_R(s) \in \mathcal{R}_j]\,|I(N(s))\right)$$

$$= p_k(I(N_R(s)))\,p_k(I(N_L(s)))\ +\ p_i(I(N_R(s)))\,p_j(I(N_Ls))) \tag{4}$$

where $\{i,j\}$ can be intendical. Then, the probability of a pixel s being at the boundaries of k region, given a neighborhood partition $N(s)$ is defined as

$$p_{B_k}(s) = \frac{p(I(N(s))|B_k)}{p(I(N(s))|B_k) + p(I(N(s))|\bar{B}_k)} \tag{5}$$

Given the definition of the probability for a pixel s being a k boundary point, the next problem is to define the neighborhood partition. We consider four different partitions of the neighborhood (the vertical, the horizontal and the two diagonals) [**fig. (3.b)**]. These partitions can be obtained by assuming four different orientations $\left[\theta = \left\{0, \frac{\pi}{4}, \frac{\pi}{2}, \frac{3\pi}{4}\right\}\right]$; it has been found experimentally that the optimal neighborhood regions are 3×3 directional windows. The use of 1×1 windows creates quite instable measurements, while the use of 5×5 windows smoothes significantly the region boundaries. We estimate the boundary probability by using the mean values over these windows, and we generate the vector:

$$B_k(s,\theta) = \left[p\left(B_k|I(...),0\right),\quad p\left(B_k|I(...),\frac{\pi}{4}\right),\quad p\left(B_k|I(...),\frac{\pi}{2}\right),\quad p\left(B_k|I(...),\frac{3\pi}{4}\right)\right]$$

where the vector elements correspond to the boundary probabilities with respect to the different neighborhood partitions. Then, the boundary information $[p_{B,k}(s)]$ for the given pixel s with respect to the k region is determined by the highest component value of the boundary information vector $B_k(s,\theta)$. The same procedure is followed for all regions, given
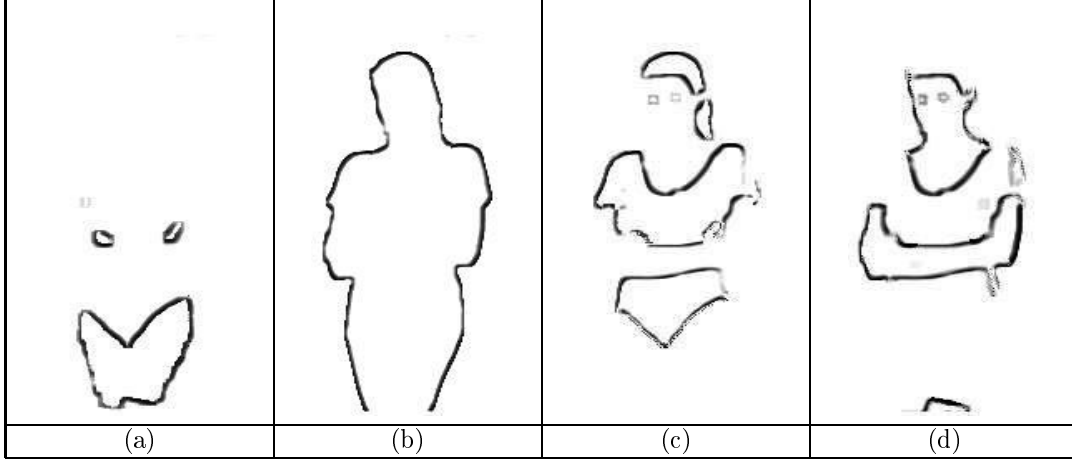
Figure 4: Boundary information with respect to the different regions for the woman image [**fig.** (2.a)]. (a) *Region 1 (black pants)*, (b) *Region 2 (background)*, (c) *Region 3 (hair, t-shirt)*, (d) *Region 4 (skin)*.

their intensity properties (Gaussian component) resulting on N boundary-based information images $[p_{B,k}(s) : k \in [1, N]]$. A demonstration of the extracted boundary information using this framework can be found in [**fig.** (4)].

Practically, the pixel-wise boundary information is estimated as follows: Initially, this information for all pixels and for all hypotheses is equal to *zero* $[\forall i \in [1, N] : p_{B,i}(s) = 0]$. Then, for each pixel, the four possible neighborhood partitions are considered. Moreover, for each partition the probabilities for the two local regions with respect to the different region hypotheses are estimated. Then, the most probable labeling assignments $[h_l, h_r]$ with respect to the local regions (left, right) are considered:

  i. If these assignments refer to the same hypothesis $[h_l = h_r]$, then the existing estimates of the boundary information are not affected,

  ii. On the other hand, if these assignments are different $[h_l \neq h_r]$ then the temporal boundary probabilities with respect to these two $[h_l, h_r]$ hypotheses are given by

$$\hat{p}_{B,t_l}(s) = \hat{p}_{B,t_r}(s) = \frac{p_{t_l}(I(N_L(s)))\, p_{t_r}(I(N_R(s)))}{\underbrace{p_{t_l}(I(N_L(s)))\, p_{t_r}(I(N_R(s)))}_{boundary\ probability} + \underbrace{p_{t_x}(I(N_L(s)))\, p_{t_x}(I(N_R(s)))}_{non-boundary\ probability}}$$

where the conditional non-boundary probability is the one that maximizes the joint probability of the two local regions given the observation set $I(N_R(s))$, and is given

by

$$\{x \in \{l, r\} : \mathbf{max}_x \left[p_{t_x}(I(N_L(s))) p_{t_x}(I_i(N_R(s))) \right]\}$$

If these boundary probabilities $[\hat{p}_{B,t_l}(s), \hat{p}_{B,t_r}(s)]$ are superior to the existing ones $[p_{B,t_l}(s), p_{B,t_r}(s)]$, then, they are used to update the old ones

$$p_{B,t_l}(s) = \hat{p}_{B,t_l}(s), \quad p_{B,t_r}(s) = \hat{p}_{B,t_r}(s).$$

Finally, the boundary information with respect to the k hypothesis for a given pixel s is given by the density function $[p_{B,k}(s)]$. However, this information can be combined using other boundary-based information sources (high gradient values, etc.).

3.2   Setting the Region Information

As far the region-information is concerned, it can be expressed directly from the Gaussian elements of the mixture model $[p_i()]$ estimated in the observed image $[p_i(I(s))]$.

3.3   Setting the Energy

Then, the segmentation task can be considered within the geodesic active region framework. According to this model the best segmentation map is determined using a set of regular curves, where each curve $[\partial \mathcal{R}_i]$:

  i. Is attracted by the boundaries of a specific region $[\mathcal{R}_i]$,

  ii. Defines an interior region with maximum joint segmentation probability given the observed intensities and the expected ones $[p_i()]$.

This map is obtained by minimizing following objective function,

$$\begin{cases} E(\mathcal{P}(\mathcal{R})) = \alpha \sum_{i=1}^{N} \iint_{\mathcal{R}_i} \underbrace{-\mathbf{log}\left(p_i\left(I(x,y)\right)\right)}_{region\ fitting} dxdy + \\ \\ \qquad (1-\alpha) \sum_{i=1}^{N} \int_{0}^{1} \underbrace{g\left(p_{B,i}\left(\partial \mathcal{R}_i(c_i)\right), \sigma_B\right)}_{boundary\ attraction} \underbrace{|\partial \dot{\mathcal{R}}_i(c_i)|}_{regularity\ constraint} dc_i \end{cases} \tag{6}$$

where

  - $\partial \mathcal{R}_i(c_i)$ is a parameterization of the region $\mathcal{R}_i$ boundaries into a planar form,

  - and $g(x, \sigma_B)$ is a Gaussian function: $\left[g(x, \sigma_B) = \frac{1}{\sqrt{2\pi}\sigma_b} e^{-\frac{x^2}{2\sigma_B^2}} \right]$.

Within this framework the set of the unknown variables consists of the the different region boundaries (curves) $[\partial \mathcal{R}_i]$. Let us now try to interpret the defined objective function, which is composed of $2N$ terms (N regions, two terms for each region). For each region $\mathcal{R}_i$, it aims at finding a curve $\underline{\partial \mathcal{R}_i}$ with the following properties:

- **Regularity**

  It is regular and smooth,

- **Region Fitting**

  It defines an interior region, that is composed of pixels with observed intensity properties close to the expected ones that are determined by the distribution $[p_i()]$.

- **Boundary Attraction**

  It is attracted by pixels which belong to the real region boundaries of $\mathcal{R}_i$. These boundaries are determined using the i conditional boundary probability $[p_{B,i}()]$.

3.4 Minimizing the Energy

The defined objective function is minimized using a gradient descent method. Thus, the system of the Euler-Lagrange motion equations with respect to the different curves (one for each region) is given by:

$$
\begin{cases}
\forall\, i \in [1,N], \\[2mm]
\dfrac{\partial}{\partial t}\partial \mathcal{R}_i(c_i) = -\,\alpha \; \underbrace{\mathbf{log}\left[\dfrac{p_i(I(\partial \mathcal{R}_i(c_i)))}{p_{k_i}(I(\partial \mathcal{R}_i(c_i)))}\right]\mathcal{N}_i(\partial \mathcal{R}_i(c_i))}_{Region-based\ force} \; + (1-\alpha) \\[6mm]
\underbrace{(g(p_{B,i}(\partial \mathcal{R}_i(c_i)),\sigma_B)\mathcal{K}_i(\partial \mathcal{R}_i(c_i)) + \nabla g(p_{B,i}(\partial \mathcal{R}_i(c_i)),\sigma_B)\cdot \mathcal{N}_i(\partial \mathcal{R}_i(c_i)))\mathcal{N}_i(\partial \mathcal{R}_i(c_i))}_{Boundary-based\ force}
\end{cases}
$$

$$(7)$$

where $\mathcal{K}_i$ (resp. $\mathcal{N}_i$) is the Euclidean curvature (resp. normal) with respect to the curve $\partial \mathcal{R}_i(c_i)$.

Moreover, the assumption that **the pixel $\partial \mathcal{R}_i(c_i)$ lies between the regions $\mathcal{R}_i$ and $\mathcal{R}_{k_i}$ was done implicitly** to provide the above motion equations which are composed of two forces, both acting in the direction of the inward normal:

i. A region-based force that aims at moving the curve towards the direction that maximizes the *a posteriori* segmentation probability. Thus, if the propagation of curve $\partial \mathcal{R}_i$ is considered and s is one of its pixel, then:

- If this pixel really belongs to $\mathcal{R}_i$, then this force is negative and aims at expanding the curve

$$s \in \mathcal{R}_i \Rightarrow p_i(I(s)) > p_{k_i}(I(s)) \Rightarrow \frac{p_i(I(s))}{p_{k_i}(I(s))} > 1 \Rightarrow -\alpha \log \left[\frac{p_i(I(s))}{p_{k_i}(I(s))} \right] < 0,$$

- While, if this pixel does not belong to $\mathcal{R}_i$, then this force is positive and aims at shrinking the curve

$$s \in \mathcal{R}_{k_i} \Rightarrow p_i(I(s)) < p_{k_i}(I(s)) \Rightarrow \frac{p_i(I(s))}{p_{k_i}(I(s))} < 1 \Rightarrow -\alpha \log \left[\frac{p_i(I(s))}{p_{k_i}(I(s))} \right] > 0.$$

i. And, a boundary-based force that aims at shrinking the curve towards the region boundaries constrained by the curvature. This force is composed of sub-forces:

- The first moves the curves towards the region boundaries, constrained by the curvature,

- While the second adjusts the curve towards the real region boundaries (the curvature does not affect this term).

The above system of equations relies on a multi-phase curve propagation (one for each region), where the interaction between the different curves is obtained thanks to the region-based term.

4   Implementation Issues

The obtained motion equations can be implemented using a Lagrangian approach, where we produce equations of motion for the position vector $\partial\mathcal{R}(c, t)$, and then updating these position using difference approximation scheme. However, there are several problems with this approach. The main problem is that the evolving model is not capable to deal with topological changes of the moving front.

This can be avoided by introducing the work of Osher and Sethian [33]. The central idea is to represent the moving front $\partial\mathcal{R}(c, t)$ as the zero-level set $\{\phi(\partial\mathcal{R}(c, t), t) = 0\}$ of a function ϕ. This representation of $\partial\mathcal{R}(c, t)$ is implicit, parameter-free and intrinsic. Additionally, it is topology-free since different topologies of the zero level-set do not imply different topologies of ϕ. It easy to show, that if the moving front evolves according to

$$\frac{\partial}{\partial t}\partial\mathcal{R}(c, t) = F(p)\,\mathcal{N}$$

for a given function F, then the embedding function ϕ deforms according to

$$\frac{\partial}{\partial t}\phi(p, t) = F(p)\,|\nabla\phi(p, t)|$$

For this level-set representation, it is proved that the solution is independent of the embedding function ϕ, and in most of the ases is initialized as a signed distance function.

Thus, the system of motion equations that drives the curve propagation for segmentation is transformed into a system of surfaces evolution given by,

$$\begin{cases} \forall\ i \in [1, N], \\ \dfrac{\partial}{\partial t}\phi_i(s) \quad = \quad -\alpha\mathbf{log}\left(\dfrac{p_i(I(s))}{p_{k_i}(I(s))}\right)\ |\nabla\phi_i(s)|\ + \\ \qquad\qquad\qquad (1-\alpha)\left(g(p_{B,i}(s),\sigma_B)\mathcal{K}_i(s)\ |\nabla\phi_i(s)| + \nabla g(p_{B,i}(s),\sigma_B)\cdot\nabla\phi_i(s)\right) \end{cases} \tag{8}$$

The main assumption that has been considered to obtain these equations is that a given pixel s of the i curve lies between the regions i and k_i. However, the region $\mathcal{R}_{k_i}$ might not be known during the evolution of the level set function ϕ_i. Hence, a temporal assignment is required to continue the evolution process. This issue can be dealt with by assuming that the region k_i is the one that corresponds to the most probable hypothesis [3], different from i.

Thus, the hypothesis k_i is determined by seeking the hypotheses set $\{j \in [1, N]\}$ and estimating the conditional probabilities $[p_j(I(s))]$ according to the observed value $I(s)$. Then, the hypothesis that is different from i and presents the maximum conditional probability is selected.

Moreover, analyzing the motion equations (7,8), some hidden problems might be observed due to the fact that the region forces are estimated using a single intensity-based probability value. This force seems to be plausible, since in the ideal case, the Gaussian components do not overlap and the segmentation decision can be taken with a lot of precision. However, for real image segmentation cases this situation is met very rare, since the most common case refers to slightly overlapping Gaussians, while the worse to Gaussians with close mean values and different variances. Furthermore, due to presence of noise, isolated intensity values incoherent with the region properties can be found within it. As a consequence, it is quite difficult to categorize a pixel, based on its very local data (single intensity value).

To cope with these problems, a circular window approach can be used, as proposed in [43]. Hence, a centralized window $W(s)$ of m pixels is defined locally around s and the probability term $[p_i(I(s))]$ is replaced with the joint probability $\left[\prod\limits_{v\in W(s)} p_i(I(v))\right]$ within the local window. Hence, the objective function is modified as,

---

[3]This assumption also is not always valid since there are cases where due to the initial curve conditions, a pixel is not attributed to any region or it lies between two regions where the second is not the most probable one. However, an alternative method to define the $p_{k_i}(I(s))$ region probability will be presented later.

$$
\begin{cases}
E(\mathcal{P}(\mathcal{R})) \; = (1-\alpha) \; \sum_{j=1}^{N} \int_{0}^{1} g\left(p_{B,i}(\partial \mathcal{R}_i(c_i)), \sigma_B\right) \left|\partial \dot{\mathcal{R}}_i(c_i)\right| dc_i \; + \\[2ex]
\qquad\qquad \alpha \; \sum_{j=1}^{N} \iint_{\mathcal{R}_j} \left[\frac{1}{|W|} \iint_{W(x,y)} -G_{x,y}(u,v)\mathbf{log}\left(p_i\left(I(u,v)\right)\right) dudv \right] dxdy
\end{cases}
\tag{9}
$$

where the function $G_{x,y}(u,v)$ follows a Gaussian form and accounts for the distance of the pixel (u,v) from the window center (x,y). This function gives more importance to the pixels that are close to the window center, while the pixels that are far away from the actual position are less considered. Moreover, this function is inversely proportional to the geometric distance from the window center. Finally $|W|$ is a normalized constant given by $\left[|W| = \sum_{(u,v)\in W(x,y)} G_{x,y}(u,v)\right]$.

The interpretation of the above objective function is the same with the one in [**eqn. (6)**]. The main difference is that the pixel-wise region probabilities have been substituted by block-wise region probabilities (weighted sum). These modifications drive to the following system of level set evolution equations:

$$
\begin{cases}
\forall \; i \in [1, N], \\[2ex]
\dfrac{\partial}{\partial t}\phi_i(s) \;\; = \;\; -\alpha \left(\dfrac{1}{|W|} \sum_{u\in W(s)} G_s(u) \left[\mathbf{log}\left(\dfrac{p_i(I(u))}{p_{k_i}(I(u))}\right)\right] \right) \; |\nabla \phi_i(s)| \; + \\[3ex]
\qquad\qquad (1-\alpha) \left(g(p_{B,i}(s), \sigma_B)\mathcal{K}_i(s) + \nabla g(p_{B,i}(s), \sigma_B)\cdot \dfrac{\nabla \phi_i(s)}{|\nabla \phi_i(s)|} \right) \; |\nabla \phi_i(s)|
\end{cases}
\tag{10}
$$

However, by adopting this approach, the model is strongly affected by the window size. Moreover, the region-based information becomes completely unreliable at the region boundaries due to use of probabilities sum over pixels that correspond to different hypotheses. Experimentally, it has been observed that the most probable assignment for the boundary windows is the one that lies between the two real hypotheses that compose the window (in term of intensity properties). To deal with this problem, a penalization of the region term for a given hypothesis might be performed for the pixels that belong to the boundaries of another hypothesis. A more elegant solution will be presented later where the idea of a "circular" window is adopted in the context of a multi-scale approach.

Then, the segmentation phase is performed as follows: A set of N initial curves is given (on for each region) and the Geodesic Active Region model is activated under a level set implementation to perform segmentation using boundary and region-based forces.

The form of these curves as well as their position is a relatively free selection. As it concerns their form (single or multiple components), there is not limitation. On the other hand their position is slightly restricted, since we demand that for each region a part of it

belongs to the interior area of the corresponding initial curve. For cases where a region is composed of multiple components, we demand that a part of each component belongs to the interior area of the initial curve. Although, this demand seems to be very strong, it can be easily met either by initializing all curves at the borders of the frame, or by generating multi-component initial curves with a large number of small areas spoiled randomly at the image.

The performance of the proposed method is demonstrated in [**fig.** (15,16,17)]. The level set multi-phase evolution is implemented using the Narrow Band approach [1, 11]. In [**fig.** (15)] all the curves are initialized at the borders of the image. On the other hand, a random initialization step is used in [**fig.** (16,17)], with a large number of overlapping spoiled sub-regions. The propagation of the curves is shown in [**fig.** (16)], while the evolution of the segmentation maps in [**fig.** (17)].

Based on the obtained results, some remarks concerning the behavior of the proposed method can be extracted. Topological changes because of the level set implementation are naturally handled, hence a number of curves can be the output of a single initial curve (splitting), or a single curve can be the output of a multi-component initial curve (merging). This is a very important property of the proposed method, since it liberates the model from the initial conditions, while splitting and merging are performed automatically without introducing any special procedures.

The obtained system of motion equations can provide a very accurate solution to the segmentation problem. Although, that the coupling between the different curves (level set functions) is performed thanks to the region-based term and is derived from the observation set, it does not use any information regarding the position of the other curves. Hence, image pixels at the same time instant might be attributed to several regions, without being constrained by the model. Additionally, an image pixel can stay un-labeled without being attributed to any region. For obvious reasons, these situations are completely undesirable and is not appropriate to tolerate them. Hence, to deal with these problematic situations, a special "coupling" procedure has to be introduced. This can be done by introducing some ideas of the work proposed in [41].

5   Coupling the Level Sets

The use of the level set theory provides a very elegant tool to propagate curves, where their position is recovered by seeking for the zero crossing points. Moreover, using this function we can decide if a given pixel either belongs to the interior curve region (negative level set value), or to the exterior one (positive value). Thus, given an pixel location, we can determined very fast the number and the nature of regions in which it belongs. Finally, if the level set function is defined as the distance function from the curve, then a step further can be done by estimating the distance of the given pixel from each curve. This information might be very valuable during the multi-phase curve propagation cases, where the overlapping between the different curves should be prohibited.

However, the overlapping between the different curves is almost an inevitable situation at least during the initialization step. Moreover, the case where an image pixel in not been attributed to any hypothesis may occurs. Let us now assume that a pixel is attributed initially to two different regions (there are two level set functions with negative values at it). Then, a constraint that discourages a situation of this nature can be easily introduced, by adding a force (alway in the normal direction) on the corresponding level set motion equations that penalizes pixels with multiple labels (they are attributed to several regions). Additionally, a similar force can be introduced which discourages situation such as pixel with no label (they do not belong to any region). This can be done by modifying the motion equations [**eqn.** (10)] as,

$$
\begin{cases}
\forall \ i \in [1, N], \\[4pt]
\dfrac{\partial}{\partial t}\phi_i(s) \ = \ \beta \underbrace{\sum_{j \in [1,N]} H_i(i, \phi_j(s)) \ |\nabla \phi_i(s)|}_{\textbf{Coupling force}} - \\[20pt]
\qquad \gamma \underbrace{\left[\mathbf{log} \left(\dfrac{p_i(I(s))}{p_{k_i}(I(s))} \right) \right] \ |\nabla \phi_i(s)|}_{Region \ Force} + \\[20pt]
\qquad \delta \underbrace{\left(g(p_{B,i}(s)|\sigma_B)\mathcal{K}_i(s) + \nabla g(p_{B,i}(s), \sigma_B) \cdot \dfrac{\nabla \phi_i(s)}{|\nabla \phi_i(s)|} \right) \ |\nabla \phi_i(s)|}_{Boundary \ force}
\end{cases}
\tag{11}
$$

where β, γ, δ are positive constants $[\beta + \gamma + \delta = 1]$, and the function $H_i(, \phi())$ is given by

$$
H_i(m, \phi_n(s)) = \begin{cases}
0, \ \text{if} \quad m = i \\
-sign(\phi_j(s)), \ \text{if} \quad m \neq i
\end{cases}
\tag{12}
$$

Let us now interpret the new artificial force that has been added to the motion equation i, for a given pixel s:

Expanding Effect:

If this pixel does not belong to any region, (the corresponding level set values at s are positive for all level set functions), then the new force is negative, equal to $f_c = -(N-1)|\nabla \phi_i|$ and aims at expanding the region $\mathcal{R}_i$ to occupy this pixel (appearance of non-attributed pixels is discouraged).

Shrinking Effect:

On the other hand, if this pixel has been already attributed to another region $[\mathcal{R}_k]$, then the corresponding level set function $[\phi_k]$ will contribute with a positive force that aims at shrinking locally the region $\mathcal{R}_i$ (the overlapping is discouraged).

Although that the selection of the function $[H_i(\phi())]$ seems to be proper, it introduces some problems. Thus, the not-attributed pixels are penalized with the same manner similarly
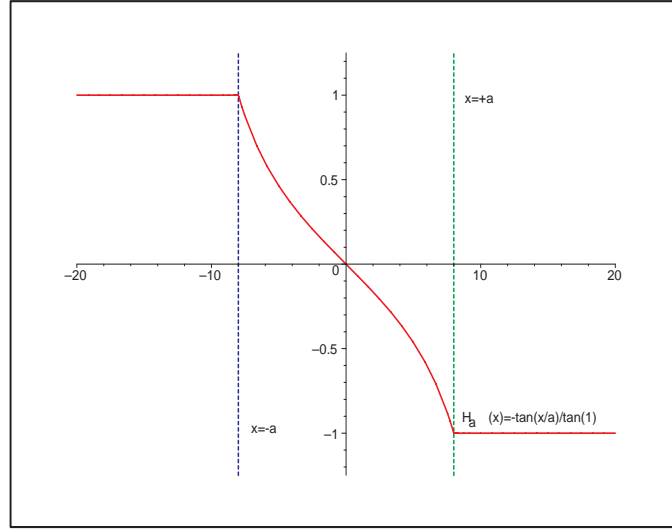
Figure 5: The trigonometric basis of the level set coupling function.

with the ones that have been attributed to multiple regions. Moreover, their distance values from the corresponding curves are not considered and hence valuable information is lost. Finally, the defined coupling function is discontinuous which is a not desirable property since it creates stability problems during the level set evolution.

To summarize, the coupling function has to be redefined by taking into account the following considerations:

i. A pixel that is already attributed to a region j and is far away from $\partial\mathcal{R}_j$, should strongly discourage the evolution of the level set $\phi_i()$ to include this pixel in $\mathcal{R}_i$,

ii. On the other hand, a pixel which belongs to the region $\mathcal{R}_j$ and is close to its boundaries (small level set value $\phi_j()$), can be reached or be liberated by $\partial\mathcal{R}_j$ during the next few iterations, and hence, the coupling force should be less powerful and "tolerate" a temporal overlapping.

Thus, inspired by the properties of the trigonometric functions, the following function that is going to be used as basis for coupling force [**fig.** (5)] is defined

$$H_a(x) = - \begin{cases} +1, & \text{if} \quad x > a \\ -1, & \text{if} \quad x < -a \\ \frac{1}{\tan(1)} \tan\left(x/a\right), & \text{if} \quad |x| \le a \end{cases} \tag{13}$$

with $a \in \mathcal{R}^+$. This trigonometric function is the basis of the coupling force given by,

$$H_i(j, \phi_j(s)) = \begin{cases} 0, & \text{if } j = i \\ H_a(\phi_j(s)), & \text{if } j \neq i \text{ and } \phi_j(s) \geq 0 \\ \frac{1}{N-1} H_a(\phi_j(s)), & \text{if } j \neq i \text{ and } \left[\cap_{\{k=1, k \neq i\}}^N \phi_k(s) > 0 \right] \end{cases} \quad (14)$$

To interpret this force via the new function, a level set function $\lfloor \phi_i() \rfloor$ and a pixel location $\lfloor s \rfloor$ are considered,

i. If s is already attributed to another region, then there is an hypothesis j for which $\phi_j(s) \leq 0$ which will contribute with a positive value (shrinking effect) to the coupling force,

$$\phi_j(s) \leq 0 \Rightarrow H_i(j, \phi_j(s)) = H_a(\phi_j(s))$$

$$\Rightarrow H_i(j, \phi_j(s)) = \begin{cases} +1, & \text{if } x < -a \\ -\frac{1}{\tan(1)} \tan(x/a), & \text{if } |x| \leq a \end{cases}$$

Furthermore, its contribution is proportional to the distance from the curve $\partial \mathcal{R}_j$ which is a very desirable property because if the given pixel is far away from the curve $\partial \mathcal{R}_j$, then, it will remain for a certain number of iterations under the occupation of $\mathcal{R}_j$. Hence, the level set function ϕ_j has to strongly discourage the attribution of this pixel to the region $[\mathcal{R}_i]$. On the other hand, if the distance is small, then it is possible that the curve $\partial \mathcal{R}_j$ will liberate this pixel soon, thus the coupling force should be less powerful.

ii. A similar interpretation can be done if this pixel is not attributed to any region.

$$\phi_j(s) \geq 0 \Rightarrow H_i(j, \phi_j(s)) = \frac{1}{N-1} H_a(\phi_j(s))$$

$$\Rightarrow H_i(j, \phi_j(s)) = \frac{1}{N-1} \begin{cases} 1, & \text{if } x > a \\ -\frac{1}{\tan(1)} \tan(x/a), & \text{if } |x| \leq a \end{cases}$$

However, for this case the coupling force has to be normalized because is not appropriate to penalize with the same way the situation of overlapping and the case in which the given pixel is not attributed to one of the regions. At the same time this force is plausible if and only if this pixel is not attributed to any region $\left[\cap_{\{k=1, k \neq i\}}^N \phi_k(s) > 0 \right]$. Finally, it is important to note that this force allows the overlapping when the curves are located exactly at the real regions boundaries.
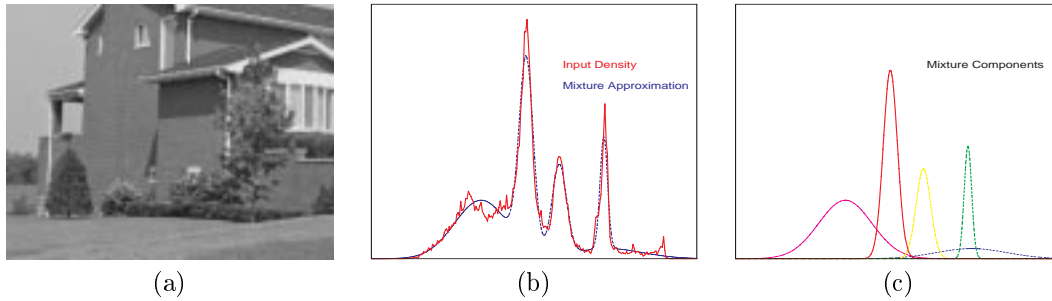
(a) (b) (c)

Figure 6: (a) Input Image, (b) Image Histogram and its approximation: *Components Number: 5, Mean Approximation Error: 2.283931e-06, Iterations Number: 421*, (c) Region Intensity Properties.

The last issue to be considered is the determination of the parameter [a] of the [$H_a()$] function. This parameter can be easily defined within the context of the *Narrow Band* level set evolution algorithm. Thus, according to this algorithm the level set evolution is performed within an active band of pixels, which are located within a zone determined by a maximum distance constraint from the latest front position. Hence, the [a] parameter can be defined using the maximum allowed distance (active band size). As a consequence, if pixel does not belong to the active band of a given level set, then this level set will contribute maximally (in terms of absolute value) to the coupling force and will strongly encourage or discourage the evolving level set to reach this pixel.

The performance of this new system of motion equations for image segmentation is demonstrated in [**fig.** (7)] for the house image [**fig.** (6)]. This image is composed of five different regions that are described/determined by strongly overlapping Gaussian functions.

The obvious constraint imposed by the coupling force is non-overlapping (at least partially) between the initial curves. When this condition is not respected, then it has been observed experimentally that the system of motion equations suffers from instability module the weight [β] of the coupling force. This problem can be resolved by modifying the weight for the coupling force as a function of time. Thus, by considering that

i. During the early states of the segmentation process the obtained map is not optimized, and the temporal overlapping should be partially tolerated,

ii. When the PDEs converge towards their asymptotic solutions [$t \to \infty$], the segmentation map is finalized and the overlapping as well as the case of non-attributed pixels should be strongly prohibited.

the weight of the coupling force is modified as follows
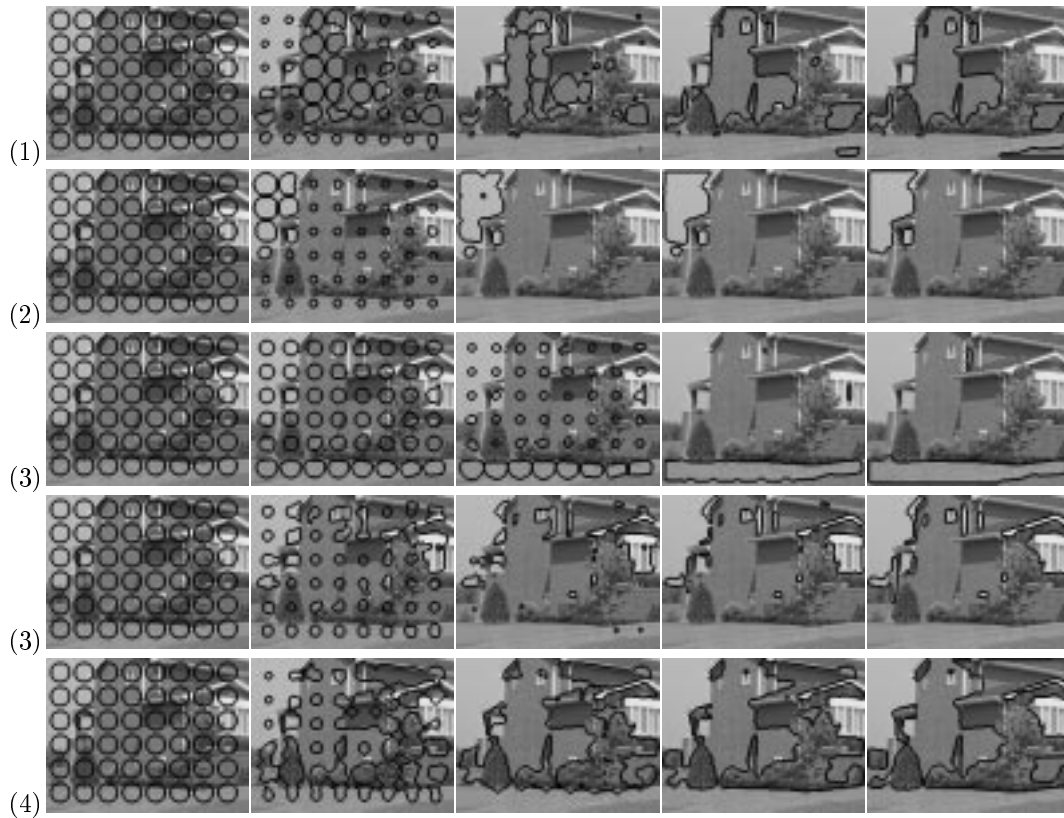
$$\beta(t) = \beta \; \frac{t}{T(\infty)} \tag{15}$$

Figure 7: The segmentation of the house image into five regions. Curve propagation: left to right. (a) House walls, (2) Sky, (b) Ground, (4) Windows, (5) Small trees, flowers, shadows $[\beta = 0.10, \gamma = 0.40, \delta = 0.50]$.

where t is the current time and $T(\infty)$ is the convergence time (this parameter is practically defined by the user by giving the iterations number). Thus, a confidence parameter has been introduced to the coupling force. This confidence is related with the current state of the segmentation procedure.

6   The final Model

The proposed method has made implicitly the assumption that the image is composed of N regions and a given pixel s lies always between two regions $[\mathcal{R}_i, \mathcal{R}_{k_i}]$. However, given
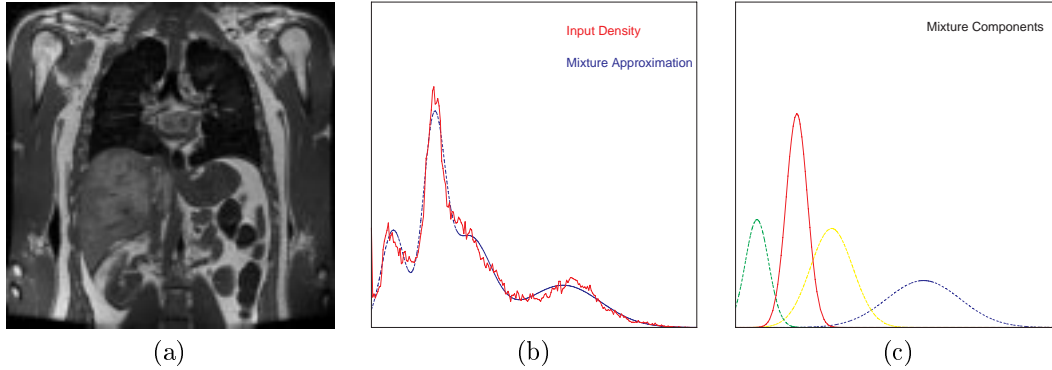
Figure 8: (a) Input Image, (b) Image Histogram and its approximation: *Components Number: 4, Mean Approximation Error: 6.279981e-05, Iterations Number: 3524,* (c) Region Intensity Properties.

the initial curves [regions] positions, some image pixels might not belong to any region. Moreover, other image pixels might be attributed to several regions.

On the other hand, during the propagation of the i curve, the region force for a given pixel s was estimated using as alternative hypothesis the most probable assignment k_i, different from i. However, this assumption is not valid if either the pixel s is attributed to an hypothesis which is not the most probable, or it is not attributed to any region.

To deal with this problem, a temporal *spending* region $\mathcal{R}_0$ has to considered. This region **(i) does not correspond to a real hypothesis** (it is composed from pixel with different hypotheses origins), **(ii) does not have a predefined intensity character** (it depends form the latest segmentation map) and **(iii) has to be empty when convergence is reached**.

These remarks indicate that a new temporal region has to be added to the objective function, as a region-based term in the following form

$$
\begin{cases}
E(\mathcal{P}(\mathcal{R})) = \alpha \sum_{i=0}^{N} \iint_{\mathcal{R}_i} -\mathbf{log}\left(p_i\left(I(x,y)\right)\right) dx dy + \\[2em]
\qquad (1-\alpha) \sum_{j=i}^{N} \int_0^1 g\left(p_{B,i}(\partial \mathcal{R}_i(c_i)), \sigma_B\right) \left|\partial \dot{\mathcal{R}}_i(c_i)\right| dc_i
\end{cases}
\tag{16}
$$

where the new region $[\mathcal{R}_0]$ is introduced. The next problem is to define the intensity properties of this region , thus the probability density function $p_0()$. This can be done by seeking the region pixels and estimating directly from the observed intensity values probability density function $p_0()$. The pixels of this region can be very easily determined within the level
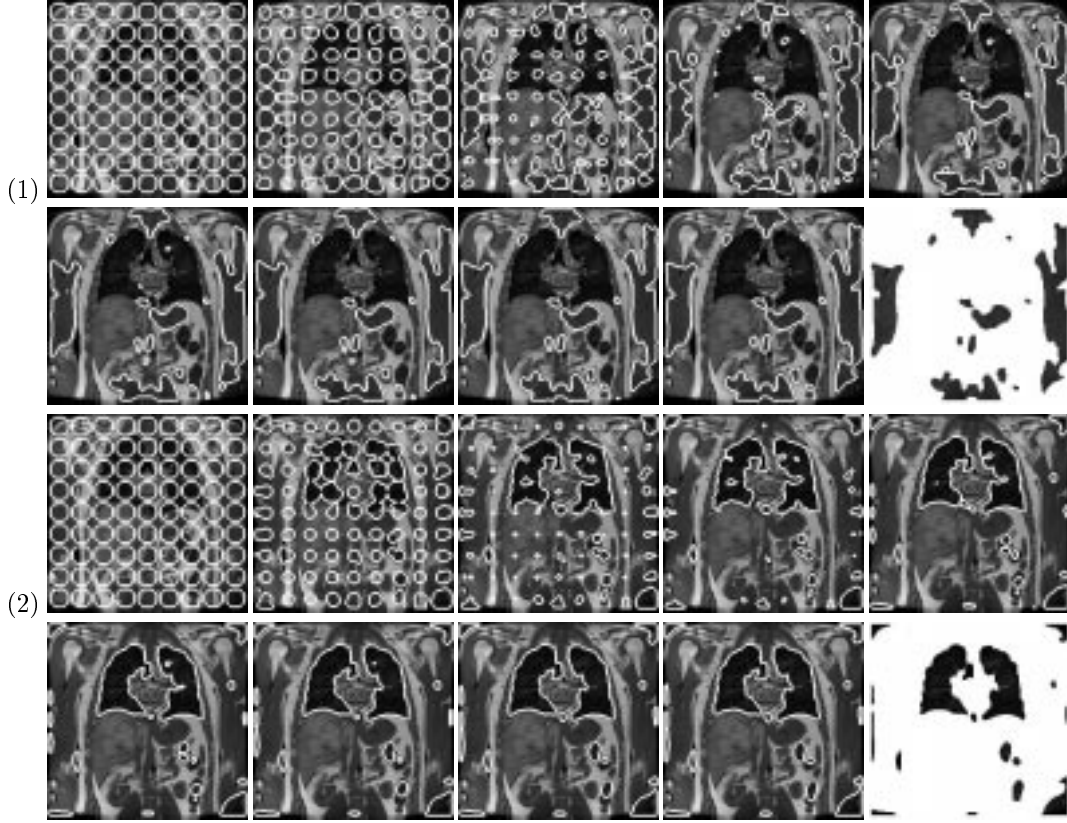
Figure 9: Segmentation for [**fig.** (8.a)] medical image:) **part 1**. (1) Region 1, (2) Region 2, $[\beta(0) = 0.33, \gamma = 0.33, \delta = 0.33]$.

set framework, since they correspond to image locations with positive level set value for all regions. Then, the minimization of the objective function leads to the following system of motion equations,

$$
\begin{cases}
\forall\ i \in [1, N], \\
\dfrac{\partial}{\partial t}\partial\mathcal{R}_i(c_i) = -\alpha \left[\mathbf{log}\left(\dfrac{p_i(I(\partial\mathcal{R}_i(c_i)))}{p_{k_i}(I(\partial\mathcal{R}_i(c_i)))} \right) \right]\ \mathcal{N}_i(\partial\mathcal{R}_i(c_i))\ + \\
\\
(1 - \alpha)\,(g(p_{B,i}(\partial\mathcal{R}_i(c_i)), \sigma_B)\mathcal{K}_i(u) + \nabla g(p_{B,i}(u), \sigma_B) \cdot \mathcal{N}_i(\partial\mathcal{R}_i(c_i)))\mathcal{N}_i(\partial\mathcal{R}_i(c_i))
\end{cases}
\tag{17}
$$

where now the probability $p_{k_i}()$ is given by,

$$p_{k_i}(s) = \begin{cases} p_0(s), & if\ s \notin \cup_{j=1,j\neq i}^{N} [\mathcal{R}_j] \\ p_m(s), & m := \mathbf{max}\{p_m(s) : m \in [1,N], m \neq i, s \in \mathcal{R}_m\} \end{cases} \tag{18}$$

and for the i motion equation is interpreted as follows:

- If the given pixel is not attributed to any region, then the spending region distribution $p_0()$ is used to determine the k_i hypothesis.

- On the other hand, if this pixel is already attributed to one, or more than one regions, then the hypothesis that gives the highest probability is selected

This system of motion equations is implemented using the level set theory, where a coupling force is also introduced,

$$\begin{cases} \forall\ i \in [1,N], \\ \dfrac{\partial}{\partial t}\phi_i(s) = \beta\left[\displaystyle\sum_{j\in[1,N]} H_i(i,\phi_j(s))\right]|\nabla\phi_i(s)| - \gamma\left[\mathbf{log}\left(\dfrac{p_i(I(s))}{p_{k_i}(I(s))}\right)\right]|\nabla\phi_i(s)| + \\ \qquad \delta\left[g(p_{B,i}(s),\sigma_B)\mathcal{K}_i(s) + \nabla g(p_{B,i}(s),\sigma_B)\cdot\dfrac{\nabla\phi_i(s)}{|\nabla\phi_i(s)|}\right]|\nabla\phi_i(s)| \end{cases} \tag{19}$$

where now the function $p_{k_i}()$ can be defined using the level set functions as follows

$$p_{k_i}(s) = \begin{cases} p_0(s), & if\ \cup_{j=1,j\neq i}^{N}[\phi_j(s) > 0] \\ p_m(s), & m := \mathbf{max}\{p_m(s) : m \in [1,N], m \neq i, \phi_m(s) \leq 0\} \end{cases} \tag{20}$$

To summarize, if a given pixel s is reached by a curve and it does not belong to any region, then this pixel is attributed to the *spending* region. On the other hand, if this pixel is already attributed to other regions, then the region with the most probable alignment given the pixel intensity is considered.

Then, the segmentation is performed as follows. Given the set of initial curve, the intensity distribution of the *spending* region is estimated. Then, a multi-phase propagation is performed using the Narrow Band algorithm. This method requires the re-initialization of the active band and the level set function when the front approaches the active band borders. During this procedure (re-initialization), the statistics of the *spending* region are updated and the processing is continued until convergence.

However, convergence might be reached with a non-empty *spending* region. This case appears when the initialization step is not "appropriate". In that case there are image regions which are never recovered by the corresponding curves. This problem might be resolved by performing a "correction" step after convergence (the curves do not propagate any more) with respect to the *spending* region. Thus, the pixels of this region are re-attributed to the other regions, and the processing is continued until convergence.
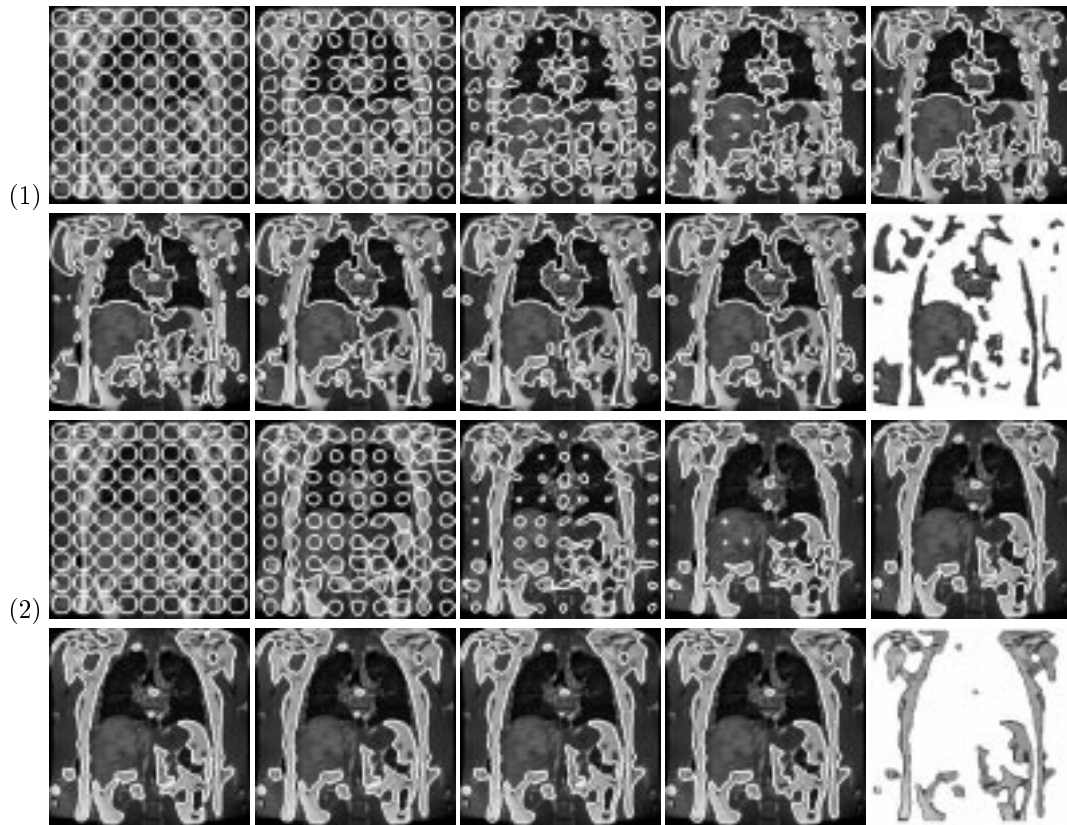
Figure 10: Segmentation for [**fig.** (8.a)] medical image:) **part 2**. (1) Region 3, (2) Region 4, $[\beta = 0.33, \gamma = 0.33, \delta = 0.33]$.

Besides, during the segmentation process we can update our statistics modules (Gaussian) with respect to the different regions. This can be done by introducing an iterative approach that uses the current segmentation output to re-estimate the region statistics, and then performs a new segmentation step (the boundary/region statistics have changed). However, in that case it is very important to obtain a relatively good segmentation map after the first step using the statistics that have been obtained using the mixture model on the observed density function. Practically, this correction step is performed once, when convergence is reached using the Gaussian components of the mixture models and aims at eliminating the errors of the global statistical modeling reflecting on a better segmentation map.
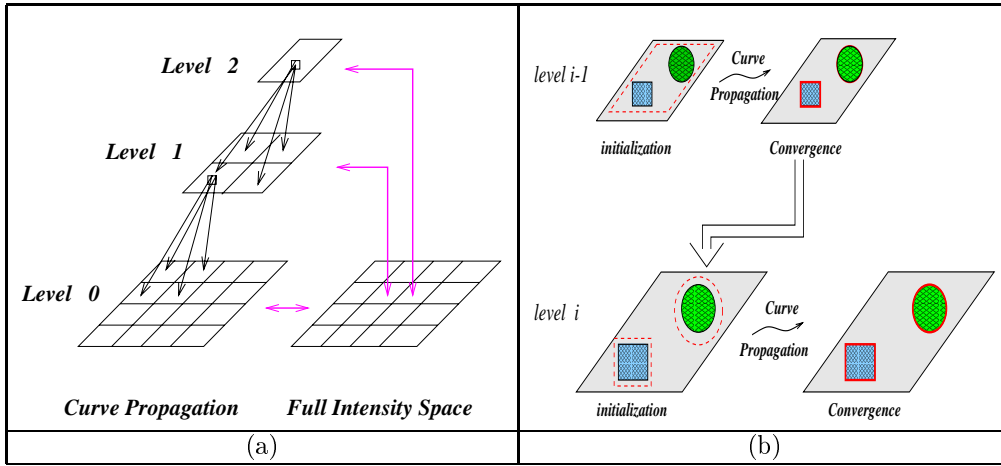
Figure 11: A Multi-Scale Approach for Image Segmentation. (a) Multi-Scale curve propagation using the full resolution data space, (b) Initialization (extrapolation) and convergence scheme at different levels.

7 Multi-scale Image Segmentation

It is well known that the use of *multi-scale* techniques reduces significantly the required computational cost of the minimization process and performs a smooth operation to the objective function that eliminates the risk of converging to local minima. These techniques have been widely used in image processing and computer vision problems with a beneficial contribution.

The main idea is to solve the minimization problem in different solution spaces, which are subsets of the original one. Thus, given a sub-space of the solution set, the solution that is adopted correspond to a set of pixels in the original space. Using a coarse to fine pyramid, an extrapolation of the solution from level with low resolution to level with finer solution configurations takes place [**fig.** (11.b)]. This extrapolation scheme is used as an initial solution for this level and a new minimization process is performed.

A rather sophisticated approach is to implement this technique consists in defining a consistent coarse-to-fine *multi-grid* contour propagation by using contours which are constrained to be piecewise constant over smaller and smaller pixel subsets [24]. The objective function which is considered at each level is then automatically derived from the original finest scale energy function. Additionally, the finest data space is used at each level, and there is no necessity for constructing a multi-resolution pyramid of the data [**fig.** (11.a)].
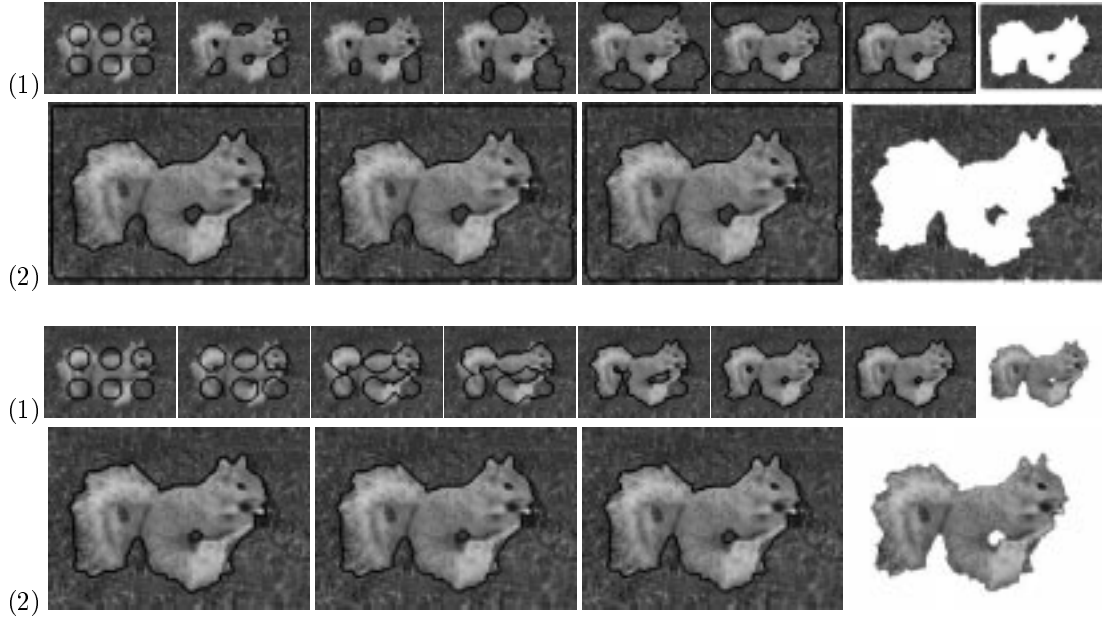
Figure 12: Multi-scale segmentation of the squirrel image into two regions. Curve propagation: left to right. (1) Level 1, (2) Level *0* (full resolution level). The final segmentation map at level 1 is used to determined the initial curve conditions at level *0*. The convergence at level *0* is achieved very fast (*2-3* iterations; for level *1*, *50* iterations are required).

We define the system of corresponding objective functions at level L as:

$$
\begin{cases}
E^L(\mathcal{P}(\mathcal{R}^L)) = \alpha \sum_{i=0}^{N} \iint_{\mathcal{R}_i^L} \left[\iint_{W^L(x,y)} -\mathbf{log}\left(p_i\left(I(u,v)\right)\right) \right] dxdy + \\
\qquad\qquad (1-\alpha) \sum_{i=1}^{N} \int_0^1 \left[\frac{1}{||W^L||} \iint_{W(\partial\mathcal{R}_i^L(p_i))} g\left(p_{B,i}\left(u,v\right)|\sigma_B\right) dudv \right] \left|\partial\dot{\mathcal{R}}_i^L(p_i)\right| dp_i
\end{cases}
$$
(21)

where ∂R_i^L is the region boundary of i at L level, $W^L(x,y)$ is the full resolution window that corresponds to the (x,y) pixel of level L, and $||W^L||$ is the size of this window.

This multi-scale approach overcomes the limitations of the circular window approach. At the low resolution levels, a window of probabilities is used to move the contour, where window probabilities are quite reliable. On the other hand, the boundary term is not very precise due to the performed smoothing operation. This problem is dealt when we proceed
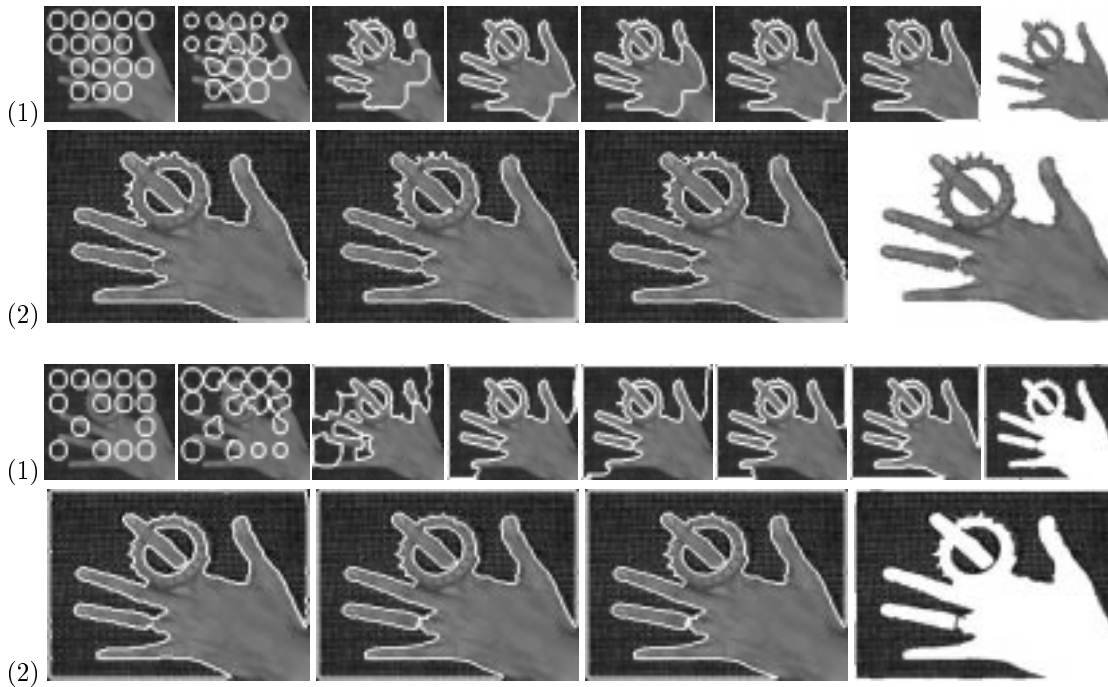
Figure 13: Multi-scale segmentation of the hand image into two regions. Curve propagation: left to right. (1) Level 1, (2) Level *0* (full resolution level). The final segmentation map at level *1* is used to determined the initial curve conditions at level 0. The convergence at level *0* is achieved very fast (*2-3* iterations; for level *1, 40* iterations are required).

from a lower resolution to a higher resolution level, because the window size gets smaller and smaller and the boundary-based term becomes more accurate. Simultaneously, at the low resolution level, we have obtained a segmentation where the noise influence has been removed, and since this result is used to initialize the operation at the next level we don't meet the noise problems that were mentioned above.

The performance of this multi-scale consideration of our model is demonstrated in [**fig.** (12,13)].

8 Discussion, Summary

In this paper, a new multi-phase level set approach for un-supervised image segmentation has been proposed. Real images of different nature (outdoor, medical, etc.) which have been

used from other segmentation approaches (woman, hand, squirrel) have been used as input to validate the proposed approach.

The obtained experimental results are very promising [**fig.** (15,7,9,10,12,13,14)]. However, an evaluation of the proposed approach is required. Three aspects are considered, namely the initialization step, the performance/contribution of the different segmentation modules, and the computational cost.

Based on the experimental results, it can be easily observed that the initial curve conditions do not constrain the model performance. However, there are some necessary conditions that have to be respected during the initialization procedure. Hence, the initial curves with respect to the different hypotheses should define image regions which include a part (even small) of the real regions that have to be recovered. To interpret this condition, let us now assume that an image sub-region $\mathcal{R}_{\{m,i\}}$ (part of the region $\mathcal{R}_m$) of the hypothesis m is completely surrounded by a sub-region of the hypothesis n. In that case, if the initial curve for m does not define an interior region that includes some pixels of $\mathcal{R}_{\{m,i\}}$, then the segmentation procedure will fail to attribute the sub-region $\mathcal{R}_{\{m,i\}}$ to the m hypothesis. This requirement can be easily met by performing a random initialization step with an important number of small spoiled regions which are randomly positioned in the image. However, such initialization steps introduce extra computational (curve propagation).

Another interesting issue refers to the evaluation of the different segmentation modules (boundary, region) and forces (boundary, region and coupling) that are used to propagate the initial curves towards the final segmentation map. Recall that the **boundary force** aims at shrinking the initial curve towards the region boundaries under a regularity constraint. Hence, if this curve defines a region which partially includes the real one (the region that has to be recovered), then the boundary force has a beneficial contribution for the curve parts that are located outside from the real region, while it discourages the curve parts that are located inside the real region to evolve towards the correct direction (outwards). However, the contribution of this force is very important. Thus, thanks to this force, **the curve is attracted very accurately by the real boundaries (an important issue for many applications,** *e.g.* **segmentation of medical images) and remains regular and smooth**. The evaluation of the **region force** is a straightforward step. This force **creates positive and negative propagation velocities that move the curve in the direction that maximizes the** *a posteriori* **segmentation probability, and liberates the model form the initial conditions**. Hence, the curve can be propagated either inwards or outwards thanks to image-based measurements which is a very nice property. Finally, the **coupling force** has a complementary contribution since it **eliminates the risk concerning the appearance of undesirable situations (not attributed pixel/attribution of a pixel to multiple regions) and increases significantly the convergence rate**.

As far the computational cost[4] is concerned, the two stages of the proposed approach will examined separately; the modeling and the segmentation phase. The modeling phase is not time consuming since the approximation of the observed histogram with a mixture

---

[4]An ULTRA-10 Sun Station have been used for all experiments with 256 MB Ram, and a processor of 299 MHZ.
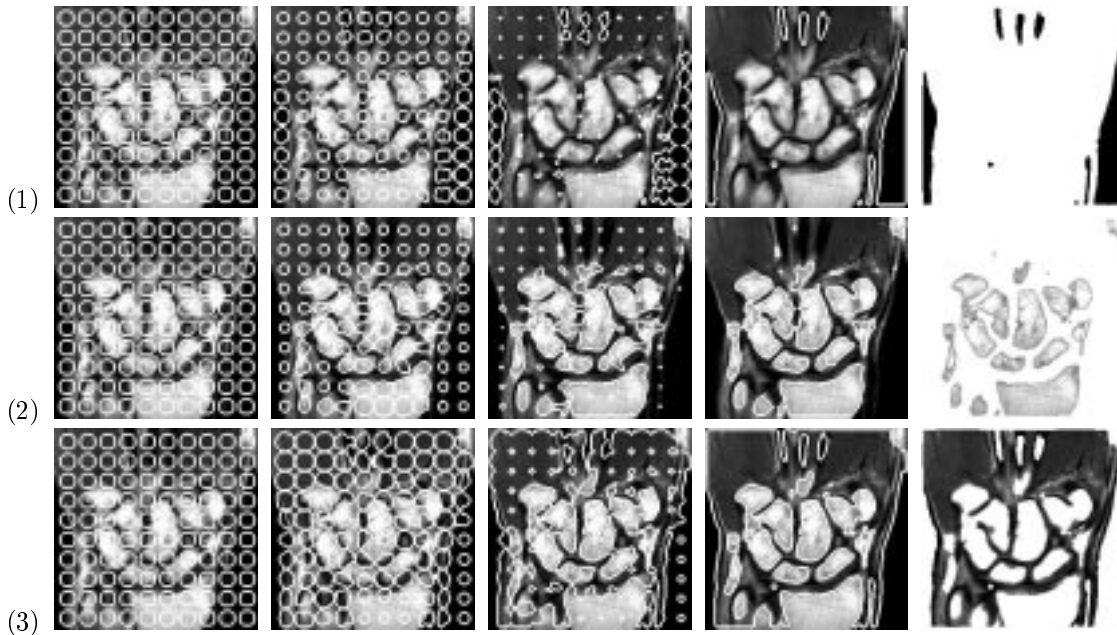
Figure 14: Segmentation for a Coronal T1 Weighted Image of the Wrist. Three different regions are detected (rows: 1,2,3). The last column corresponds to the final segmentation result with respect to the different regions projected at the image, $[\beta(0) = 0.10, \gamma = 0.50, \delta = 0.40]$.

of Gaussian elements takes less than *one* second. The segmentation phase consists of two steps; the extraction of the boundary/region information and the propagation of curves. The extraction of the region information is performed very fast, while the same procedure is time consuming as far the boundary information is concerned. Thus, according to the probabilistic boundary module, for each pixel location four different partitions are considered. Moreover, for each partition the probability values for all hypotheses have to estimated twice (left and right local region) over a 3×3 window. As a consequence, this step is time consuming especially when the image is composed of many different regions. However, to give an idea about this cost, for a 256×256 with four hypothesis, the estimation of the boundary information takes approximately 3 to 5 seconds. Moreover, the computational cost of the propagation phase can be estimated with a lot of difficulty and is strongly related with the hypotheses number (number of level set functions). Additionally, it is strongly affected by the initial curve conditions. However, by considering the experiments related with the complexity of the *Narrow Band* algorithm, some predictions can be done regarding the computational cost of the propagation phase. These predictions are not accurate and

are affected by a large number of parameters such as: initial curve conditions, hypotheses number, weights of the different segmentation modules, narrow band size, time step, etc... Thus, for a 256×256 image (Coronal image [**fig.** (14)]) with a random initialization step, the propagation phase takes approximately 20 seconds. This cost is significantly decreased by the use of the multi-scale approach (three to five times).

Summarizing, in this paper a new variational framework has been proposed to deal with the problem of image segmentation. This framework unifies boundary and region-based segmentation modules within the Geodesic Active Region model. Initially, the number of regions and their intensity properties are determined automatically by performing a statistical modeling procedure on the observed density function (image histogram). Then, the boundary information is estimated using a probabilistic edge detector, while the region-based information is expressed using conditional probabilities. Both information sources are integrated using a Geodesic Active Region-based objective function. This function is minimized using a gradient descent method resulting on a system of motion equations that deform the set of initial curves towards the boundaries of the different regions. These equations are implemented using the level set theory. Moreover, a coupling procedure is introduced between the different level set functions to increase the convergence rate and to deal with undesirable situations (pixels that are not attributed to any region, pixels that are attributed to multiple regions). Finally, to decrease the risk of convergence to local minima and to decrease the required computational cost, the proposed framework is considered in a multi-scale implementation. To summarize, the contributions of the proposed image segmentation model are the following:

- An adaptive method that determines automatically the regions number and their intensity properties,

- A variational image segmentation framework that integrates boundary and region-based segmentation modules and connects the optimization procedure with the the curve propagation theory,

- The implementation of this framework within level set theory resulting on a segmentation paradigm that can deal automatically with changes of topology and is free from the initial conditions,

- The interaction between the different curves [regions] propagation using an artificial coupling force that increases the convergence rate, and eliminates the risk of convergence to a non-proper solution,

- And, the consideration of the proposed model in a multi-scale framework, which deals with the presence of noise, increases the convergence rate, and decreases the risk of convergence in a local minimum.

As far the future directions of this work, the use of color images is a challenge. However for this case, the statistical modeling phase where the number of regions and their intensity properties are determined is more complicated since we have to deal with multi-variate

distribution. A step further is the un-supervised segmentation of textured images, using the proposed framework. Finally, there is number of practical issues to be solved like the initial curve conditions, the selection of the model parameters, etc.

References

[1] D. Adalsteinsson and J. Sethian. A Fast Level Set Method for Propagating Interfaces. *Journal of Computational Physics*, 118:269–277, 1995.

[2] R. Adams and L. Bischof. Seeded Region Growing. *IEEE Transactions on Pattern Analysis and Machine Intelligence*, 16:641–647, 1994.

[3] J. Besag. On the statistical analysis of dirty images. *Journal of Royal Statistics Society*, 48:259–302, 1986.

[4] R. Beveridge, S. Griffith, R. Kohler, R. Hanson, and M. Riseman. Segmenting Images Using Localizing Histograms and Region Merging. *International Journal of Computer Vision*, 2:311–352, 1989.

[5] C. Bouman and M. Shapiro. A multiscale random field model for bayesian image segmentation. *IEEE Transactions on Image Processing*, 3:162–177, 1994.

[6] J. Canny. A computational approach to edge detection. *IEEE Transactions on Pattern Analysis and Machine Intelligence*, 8:769–798, 1986.

[7] V. Caselles, R. Kimmel, and G. Sapiro. Geodesic active contours. In *IEEE International Conference on Computer Vision*, Boston, USA, 1995.

[8] V. Caselles, R. Kimmel, and G. Sapiro. Geodesic active contours. *International Journal of Computer Vision*, 22:61–79, 1997.

[9] A. Chakraborty, H. Staib, and J. Duncan. Deformable Boundary Finding in Medical Images by Integrating Gradient and Region Information. *IEEE Transactions on Medical Imaging*, 15(6):859–870, 1996.

[10] T. Chan and L. Vese. n Active Contour Model without Edges. In *International Conference on Scale-Space Theories in Computer Vision*, pages 141–151, 1999.

[11] D. Chop. Computing Minimal Surfaces via Level Set Curvature Flow. *Journal of Computational Physics*, 106:77–91, 1993.

[12] P. Chou and C. Brown. The theory and practice of bayesian image labeling. *International Journal of Computer Vision*, 4:185–210, 1990.

[13] C. Chu and J. Aggarwal. The integration of image segmentation maps using region and edge information. *IEEE Transactions on Pattern Analysis and Machine Intelligence*, 15:241–1252, 1993.

Figure 15: Segmentation for the woman image [**fig.** (2.a)]. Multi-phase Curve Propagation. All initial curves are located at the borders of the image. (1) *Region 1 (black pants)*, (2) *Region 2 (skin)*, (3) *Region 3 (background)*, (d) *Region 4 (hair, t-shirt)*.

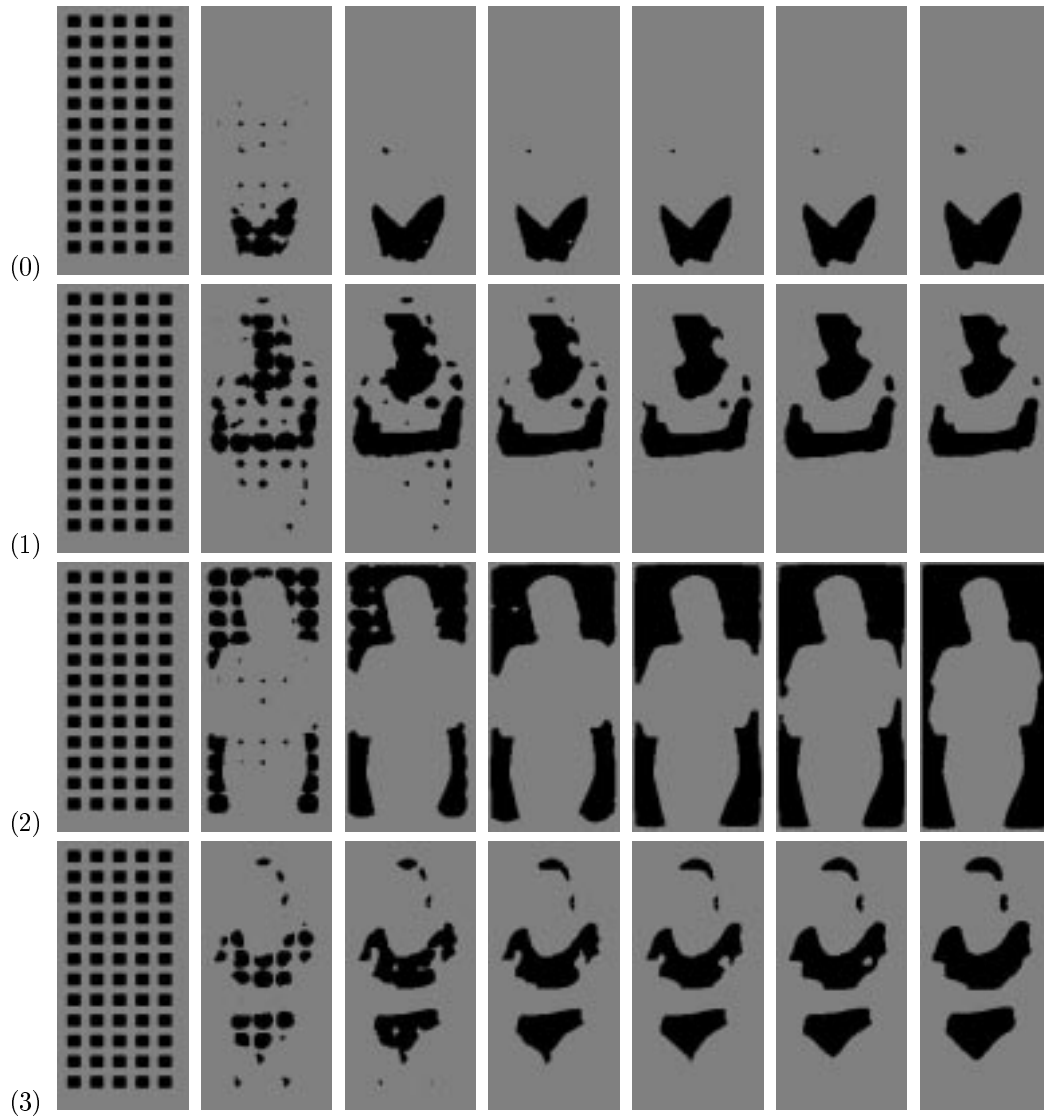Figure 16: Segmentation for the woman image [**fig.** (2.a)]. Multi-phase Curve Propagation. A random initialization step is used with a large number of spoiled regions. The initial regions are the same for all hypothesis. (1) *Region 1 (black pants)*, (2) *Region 2 (skin)*, (3) *Region 3 (background)*, (d) *Region 4 (hair, t-shirt)*.

Figure 17: Segmentation of the woman image [**fig.** (2.a)]. The evolution of the segmented regions (regions color: black). A random initialization step is used with a large number of spoiled regions. The initial regions are the same for all hypothesis. (1) *Region 1 (black pants)*, (2) *Region 2 (skin)*, (3) *Region 3 (background)*, (d) *Region 4 (hair, t-shirt)*.

[14] D. Cohen. On active contour models and balloons. *CVGIP: Image Understanding*, 53:211–218, 1991.

[15] M. Cooper. The tractability of segmentation and scene analysis. *International Journal of Computer Vision*, 30:27–42, 1998.

[16] R. Deriche. Using Canny's Criteria to Derive a Recursively Implemented Optimal edge Detector. *International Journal of Computer Vision*, 1:167–187, 1987.

[17] H. Derin, H. Elliott, R. Cristi, and D. Geman. Bayes smoothing algorithms for segmentation of binary images modeled by markov random fields. *IEEE Transactions on Pattern Analysis and Machine Intelligence*, 6:1186–1191, 1984.

[18] R. Duda and P. Hart. *Pattern Classification and Scene Analysis*. John Wiley & Sons, Inc., 1973.

[19] D. Geiger and A. Yuille. A common framework for image segmentation. *International Journal of Computer Vision*, 6:227–243, 1991.

[20] S. Geman and D. Geman. Stochastic Relaxation, Gibbs Distributions, and the Bayesian Restoration of Images. *IEEE Transactions on Pattern Analysis and Machine Intelligence*, 6:721–741, 1984.

[21] R. Grzeszczuk and D. Levin. Brownian strings: Segmenting images with stochastically deformable contours. *IEEE Transactions on Pattern Analysis and Machine Intelligence*, 19:1100–1114, 1997.

[22] J. Haddon and J. Boyce. Inage Segmentation by Unifying Region and Boundary Information. *IEEE Transactions on Pattern Analysis and Machine Intelligence*, 12:929–948, 1990.

[23] R. Haralick and L. Shapiro. Image segmentation techniques. *CVGIP: Image Understanding*, 29:100–132, 1985.

[24] F. Heitz, P. Perez, and P. Bouthemy. Multiscale minimization of global energy functions in some visual recovery problems. *CVGIP: Image Understanding*, 59:125–134, 1994.

[25] H. Ip and D. Shen. An affine-invariant active contour model (ai-snake) for model-based segmentation. *Image and Vision Computing*, 16:135–146, 1998.

[26] M. Kass, A. Witkin, and D. Terzopoulos. Snakes: Active contour models. *International Journal of Computer Vision*, 1:321–332, 1988.

[27] I. Kerfoot and Y. Bresler. Theoretical analysis of multispectral image segmentation criteria. *IEEE Transactions on Image Processing*, 8:798–820, 1999.

[28] S. Kichenassamy, A. Kumar, P. Olver, A. Tannenbaum, and A. Yezzi. Gradient flows and geometric active contour models. In *IEEE International Conference on Computer Vision*, pages 810–815, Boston, USA, 1995.

[29] A. Leonardis, A. Gupta, and R. Bajcsy. Segmentation of range images as the search for geometric parametric models. *International Journal of Computer Vision*, 14(3):253–270, 1995.

[30] R. Malladi, J. Sethian, and B. Vemuri. Shape modeling with front propagation: A level set approach. *IEEE Transactions on Pattern Analysis and Machine Intelligence*, 17:158–175, 1995.

[31] A. Mitiche and J. Aggarwal. Image segmentation by conventional and information-integrating techniques: A synopsis. *Image and Vision Computing*, 3:50–62, 1985.

[32] D. Mumford and J. Shah. Boundary detection by minimizing functionals. In *IEEE Conference on Computer Vision and Pattern Recognition*, San Fransisco, USA, 1985.

[33] S. Osher and J. Sethian. Fronts propagating with curvature-dependent speed : algorithms based on the hamilton-jacobi formulation. *Journal of Computational Physics*, 79:12–49, 1988.

[34] N. Paragios and R. Deriche. Geodesic Active regions for Motion Estimation and Tracking. In *IEEE International Conference on Computer Vision*, pages 688–674, Corfu, Greece, 1999.

[35] N. Paragios and R. Deriche. Geodesic Active regions for Supervised Texture Segmentation. In *IEEE International Conference on Computer Vision*, pages 926–932, Corfu, Greece, 1999.

[36] T. Pavlidis and Y.T. Liow. Integrating region growing and edge detection. *IEEE Transactions on Pattern Analysis and Machine Intelligence*, 12:225–233, 1990.

[37] A. Pentland. Automatic Extraction of Deformable Part Models. *International Journal of Computer Vision*, pages 107–126, 1990.

[38] C. Samson, Blanc-Féraud L., G. Aubert, and J. Zerubia. A Level Set Model for image classification. In *International Conference on Scale-Space Theories in Computer Vision*, pages 306–317, 1999. http://www.inria.fr/RRRT/RR-3662.html.

[39] K. Siddiqi, Y-B. Lauziere, A. Tannenbaum, and S. Zucker. Area and Length Minimizing Flows for Shape Segmentation. In *IEEE Conference on Computer Vision and Pattern Recognition*, pages 621–627, Puerto Rico, USA, 1997.

[40] A. Yezzi, A. Tsai, and A. Willsky. A statistical approach to curve evolution for image segmentation. In *IEEE International Conference on Computer Vision*, pages xx–yy, Corfu, Greece, 1999.

[41] H-K. Zhao, T. Chan, and S. Osher. A variational level set approach to multiphase motion. *Journal of Computational Physics*, 127:179–195, 1996.

[42] S. Zhu, T. Lee, and A. Yuille. Region Competition: Unifying Snakes, Region Growing Energy/Bayes/MDL for Multi-band Image Segmentation. In *IEEE International Conference on Computer Vision*, pages 416–423, Boston, USA, 1995.

[43] S. Zhu and A. Yuille. Region Competition: Unifying Snakes, Region Growing, and Bayes/MDL for Multiband Image Segmentation. *IEEE Transactions on Pattern Analysis and Machine Intelligence*, 18:884–900, 1996.